Influence of Surface Energetic Heterogeneity of Microporous Adsorbents on Adsorptive Separation of CO_2, CO, N_2, and H_2 from a Controlled-Combustion of Solid Wastes

M.H. Kim[*, 1], I.H. Cho[1], J.H. Park[1], S.O. Choi[2], I.S. Lee[2]

[1]Department of Environmental Engineering, Daegu University
201 Daegudae-ro, Jillyang, Gyeongsan 712-714, Korea
[2]Experiment & Research Team, Samsung-BP Chemicals Co. Ltd.
63-15 Sanggae-ro, Cheongryang, Ulju, Ulsan 689-860, Korea

Abstract

This study has been concentrated on the effect of the surface nonuniformity of microporous zeolites, activated carbons (AC), and metal-organic frameworks on the adsorption of CO_2, CO, N_2, and H_2 at 25°C and low equilibrated pressures ≤ 850 Torr. The shape of the measured isotherms for the adsorbates strongly depended on themselves as well as on the adsorbents, which could be well correlated with those electronic properties and these surface nonuniformity levels. The selectivity of CO_2 to other gases could be explained by different surface nonuniformity among the adsorbents. The zeolites with the most energetically-heterogeneous surfaces yielded high CO_2 uptakes and CO_2/CO selectivity factors at low pressures. On a surface of the ACs that possessed a moderate surface nonuniformity between the zeolites and a MOF and have minor quadrupole-adsorbent interactions, the adsorption behaviors and the selectivities showed an intermediate feature.

Introduction

Conventional microporous solids, zeolites and activated carbons, have been widely studied for adsorptive separation of CO_2 from gas mixtures with other gases, such as CH_4, CO, N_2, and H_2 [1–3], and recently, metal-organic frameworks (MOF) and zeolitic imidazolate frameworks (ZIF) are highlighted as a new outstanding adsorbent because they possess very high surface areas and their textural properties are easily tunable [4–8]. In the case of zeolitic materials, low Si/Al zeolites, such as Y and 13X, are frequently used for such a CO_2 adsorption due to a stronger affinity to this gas molecule [1,9]. Activated carbons (AC) have a variety of surface functional groups, such as carbonyl, phenol, carboxyl, lactone, and ether, and these sites after proper thermal excursion play a good role for CO_2 adsorption [1,10]. Many types of MOFs can be tailored using different metal-organic building blocks and organic linkers, and some metal centers after quest removal are responsible for CO_2 adsorption [4–7,11,12].

Cost-efficient regeneration of porous sorbents is required for adsorptive CO_2 separation and has been successfully conducted by using pressure swing techniques, such as vacuum swing adsorption (VSA) and pressure swing adsorption (PSA) [2,3]. Many VSA processes periodically repeat cycles between adsorption near 1 bar and desorption around 30 – 100 Torr [13,14], while industrial PSA systems allow adsorption at relatively higher pressures, typically 4 – 6 bar, and then desorption near 1 bar [2,9,15]. Such VSA techniques need a rather much energy compared to PSA ones; however, those provide a better separation efficiency, due to a higher working capacity that is mainly associated to a common feature of microporous materials on which adsorption of light gases with high polarizability and quadrupole moment, such as CO_2, usually approaches almost saturated coverage at low pressures [2] and after which, only a small increment occurs. This behavior is more critical for microporous solids with surface sites having high affinity to CO_2. This surface energetic heterogeneity also influences the extent of preferential adsorption of CO_2 over other gases, usually defined as selectivity.

The difference in the surface nonuniformity among adsorbents should be considered for a better working capacity and selectivity for CO_2 adsorption and can be disclosed by comparing its adsorption isotherms collected at low pressure region at which such surface features would prominently appear. Thus, this study has focused on low-pressure adsorption behavior of commercially-available zeolites, ACs and MOFs on which CO_2, CO, N_2, and H_2 were adsorbed at equilibrated pressures ≤ 850 Torr (≈ 1.13 bar). The chosen gases are a predominant component of a well-controlled gasification of biomass-based wastes.

Experimental

Zeolites used were NaY (CBV 100, Zeolyst) and NaX (Z10-08EP, Zeochem) with the respective Si/Al ratio of 2.3 and 1.3 that were independently measured using an ICP (inductively coupled plasma) spectroscopy. A Norit GCN612 and a Kansai Coke and Chemicals MSP-20 were employed as a model AC, designated to "GCN" and "MSP", respectively. Commercial MOF analogues were purchased from Aldrich: a Basolite A100 isostructural to MIL-53 (Al) and a Basolite Z1200 to ZIF-8 [4,5], designated to "A100" and "Z1200", respectively.

A Micromeritics ASAP 2020 system was used for collecting N_2 sorption data of the adsorbents at -196°C.

* Corresponding author: moonkim@daegu.ac.kr
Proceedings of the European Combustion Meeting 2015

For this, an appropriate amount of each sample, ca. 40 mg, was loaded into a BET adsorption cell following evacuation at 200°C in vacuum overnight. Textural properties of the adsorbents, such as BET surface area (S_{BET}), and micro-/mesopore size and volume, were calculated using the sorption data. The Saito-Foley cylindrical pore model was applied to micropores in all the sorbents, except for those in the ACs which were determined by the original Horvath-Kawazoe slit pore model [16,17]. The mesopores were estimated using the Barrett-Joyner-Halenda (BJH) model.

A stainless steel system with a high dynamic vacuum below 10^{-8} Torr, equipped with an Oerlikon Leybold Vacuum Model TURBOVAC 151 turbomolecular pump with a Turbo.Drive TD 20 Classic controller backed by a mechanical pump (Kodivac, GHP-340K) was used for volumetrically measuring CO_2, CO, N_2, and H_2 adsorptions on the chosen adsorbents. A single gauge controller (Pfeiffer, Model TPG 261) was employed to display dynamic vacuum levels. Gas pressure was measured using an absolute Honeywell Model Super TJE ultra precision pressure transducer (Type AP112) with a full range of 200 psi connected to a Sensys Model 1300 pressure indicator, and temperature was monitored using a digicator (Hanyoung Nux, BK-6M). Details of such a system have been provided elsewhere [18–20].

Typically 0.5 g each adsorbent was placed in a sample cell in a cylindrical electric furnace equipped with a temperature controller (Misung S&I, TC500P) and evacuated at 300°C overnight under a vacuum using the rotary vane pump following further evacuation for 1 h at room temperature using the TMP high vacuum system. Then, using a Peltier thermoelectric device with a temperature controller (Omega, Model CN 7500), the adsorption cell was controlled to be 25°C at which all adsorption measurements were conducted. During the pretreatment and gas adsorption, temperature of the sample cell was monitored using an Omega Model 410B Digicator. CO_2 (99.999%), CO (99.998%), N_2 and H_2 (99.9999%, Praxair) were further purified by flowing them through moisture traps and Oxytraps (Alltech Assoc.).

Results and Discussion

All adsorbents used had a common feature of microporous materials, based on the shape of N_2 sorption isotherms (not shown here), and the size of micropores and their occupancy, depending on them, as provided in Table 1. NaY and NaX with a faujasite framework topology has a similar d_m, and the former give somewhat higher S_{BET} value. The two ACs, i.e., GCN and MSP, consist of a microporous structure with a pore size of 5.0 - 5.5 Å and these surface areas are relatively larger. MOFs give the greatest micropore sizes, and the measured surface areas of A100 and Z1200 are very similar to or comparable with those of the respective NaY and GCN. Among the sorbents, the largest V_m value is indicated for MSP whose S_{BET} was also the highest.

Table 1
Textural properties of zeolites, ACs and MOFs used.

Adsorbent	S_{BET} (m^2/g)	d_m (Å)	Pore volume (cm^3/g)	
			V_m	V_t
NaY	847	7.9	0.31	0.34
NaX	724	7.6	0.27	0.37
GCN	1132	5.0	0.44	0.52
MSP	2508	5.5	0.99	1.29
A100	838	10.9	0.36	1.26
Z1200	1301	12.3	0.55	0.68

Note. d_m: micropore diameter; V_m: micropore volume; V_t: total pore volume.

Isotherms of CO_2, CO, N_2, and H_2 adsorptions on zeolites, ACs and MOFs at low pressure region are of particular interest because of their utilization as a VSA adsorbent. Figure 1 shows CO_2 adsorption on the porous solids at 850 Torr. At this pressure, the indicated CO_2 uptake is in the order NaY (7.98) > NaX (5.07) > MSP (4.12) > GCN (3.24) > A100 (2.56) >> Z1200 (0.98 mmol/g). Both the shape of isotherms measured volumetrically and CO_2 adsorption capacity strongly depended on the adsorbent used. Two zeolites, NaY and NaX, display a CO_2 adsorption that steeply increases up to 150 Torr and then occurs with a small increment, which is a typical character of microporous solids with high surface nonuniformity with high affinity sites for binding CO_2 [6,21,22].

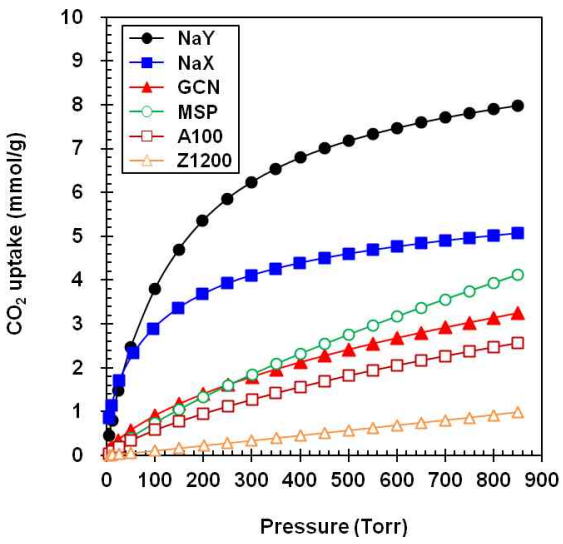

Fig. 1. Isotherms of zeolites, ACs and MOFs for CO_2 adsorption at 25°C.

Distinctive response of CO_2 adsorption to equilibrated pressures was indicated for ACs and MOFs. Not that much steep increase at such low pressure region is shown for all these samples. Two ACs and A100 give a weak character of the Langmuir isotherm;

however, Z1200 has an isotherm that is almost linear even up to 850 Torr. It is proposed that the surface of this adsorbent would be homogeneous and has few strong-binding sites even for CO_2 [2,23]. Consequently, it is clear that the surface nonuniformity of the sorbents is closely related to their CO_2 adsorption capacity.

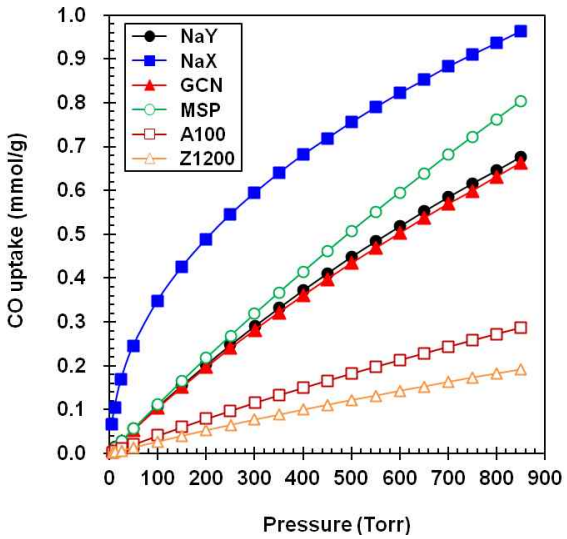

Fig. 2. Isotherms of zeolites, ACs and MOFs for CO adsorption at 25°C**.**

Similar behaviors were disclosed for CO adsorption with the six microporous sorbents, as provided in Fig. 2. A shape of the Langmuir adsorption is visible with NaX, while NaY gives a CO adsorption similar to that appeared for GCN and these isotherms suggest weak surface energetic heterogeneity. Whereas, the other adsorbents all show almost linear increase with pressure. These results are mainly due to a lower polarizability (19.5×10^{-25} cm^3) and quadrupole moment (25.0×10^{25} esu·cm^2) than those (26.5 – 29.11×10^{-25} cm^3 and 43.0×10^{25} esu· cm^2, respectively) for CO_2 [2,6,24].

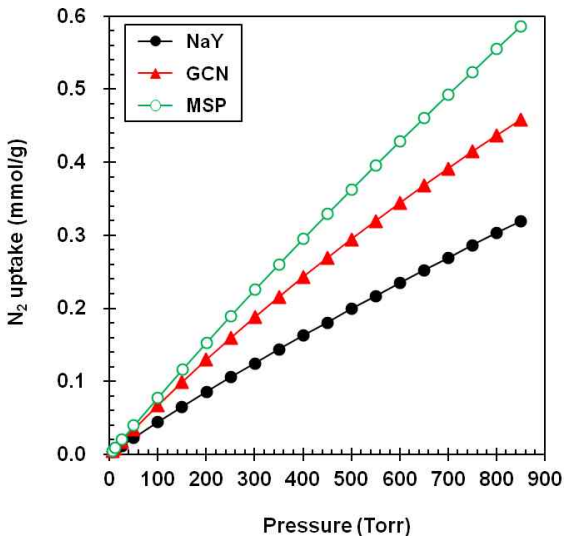

Fig. 3. Isotherms of NaY and ACs for N_2 adsorption at 25°C.

The NaY, that had revealed the highest CO_2 uptake at 850 Torr among the adsorbents studied here, and the two AC all showing higher CO_2 adsorption than the Basolites were chosen for adsorbing N_2, and H_2. As seen in Fig. 3, the carbonaceous materials give a greater CO_2 adsorption compared to the zeolite, which is in good agreement with the literature [25], implying a lower CO_2/N_2 selectivity. This suggests that they may not good adsorbent for VSA applications to gas streams with significant N_2 levels.

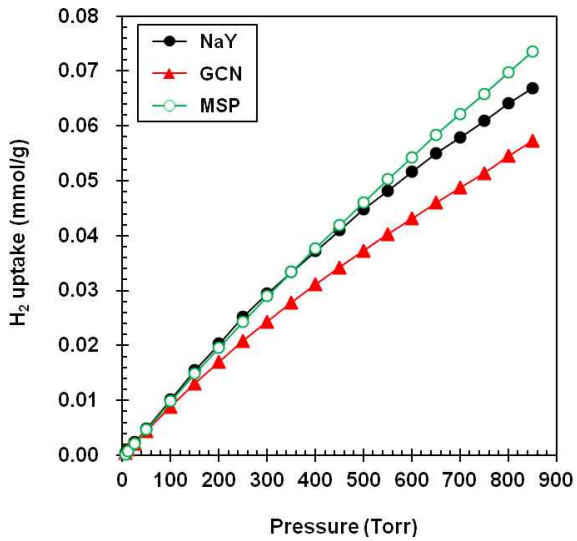

Fig. 4. Isotherms of NaY, and ACs for H_2 adsorption at 25°C.

H_2 adsorption on NaY and ACs at 25°C is displayed against equilibrated pressures in Fig. 4. The extent of its adsorption is much lower than that of CO_2 as expected, regardless of adsorbent, which is because of the lowest polarizability (8.0 – 8.042×10^{-25} cm^3) and quadrupole moment (6.62×10^{25} esu·cm^2) thereby allowing the weakest adsorbate-adsorbent interactions [2,6,24].

Conclusions

The difference in surface energetic heterogeneity among zeolites, ACs and MOFs gives distinct isotherm shape and performances in the adsorption of adsorbates, particularly CO_2 with high quadrupole moment. Zeolitic materials with an energetically wide range of adsorption sites (Na cations) for CO_2, such as NaY, may be a better adsorbent for low pressure swing applications.

Acknowledgement

This study was partly supported by the Grant # 20123010100010 of the New & Renewable Energy of the Korea Institute of Energy Technology Evaluation and Planning (KETEP).

References

[1] T.D. Pham, R. Xiong, S.I. Sandler, R.F. Lobo, Micropor. Mesopor. Mater. 185 (2014) 157–166.

[2] R.T. Yang, Adsorbents: Fundamental and Applications, John Wiley & Sons Inc., Hoboken, 2003.
[3] R. Kumar, Ind. Eng. Chem. Res. 33 (1994) 1600–1605.
[4] T. Loiseau, C. Serre, C. Huguenard, G. Fink, F. Taulelle, M. Henry, T. Bataille, G. Ferey, Chem. Eur. J. 10 (2004) 1373–1382.
[5] K.S. Park, Z. Ni, A.P. Cote, J.Y. Choi, R. Huang, F.J. Uribe-Romo, H.K. Chae, M. O'Keeffe, O.M. Yaghi, PNAS 103 (2006) 10186–10191.
[6] J.R. Li, R.J. Kuppler, H.C. Zhou, Chem. Soc. Rev. 38 (2009) 1477–1504.
[7] Y.S. Bae, R.Q. Snurr, Angew. Chem. Int. Ed. 50 (2011) 11586–11596.
[8] H. Furukawa, N. Ko, Y.B. Go, N. Aratani, S.B. Choi, E. Choi, A.O. Yazaydin, R.Q. Snurr, M. O'Keeffe, J. Kim, O.M. Yaghi, Science 329 (2010) 424–428.
[9] M. Palomino, A. Corma, J.L. Jorda, F. Rey, S. Valencia, Chem. Commun. 48 (2012) 215–217.
[10] H. Jankowska, A. Swiatkowski, J. Choma, Active Carbon, Ellis Horwood and Wydawnictwa Naukowo-Techniczne, Warsaw, 1991.
[11] J.R. Li, Y. Ma, M.C. McCarthy, J. Sculley, J. Yu, H.K. Jeong, P.B. Balbuena, H.C. Zhou, Coord. Chem. Rev. 255 (2011) 1791–1823.
[12] A.R. Millward, O.M. Yaghi, J. Am. Chem. Soc. 127 (2005) 17998–17999.
[13] N. Tlili, G. Grevillot, C. Vallieres, Int. J. Greenhouse Gas Control 3 (2009) 519–527.
[14] A.L. Chaffee, G.P. Knowles, Z. Liang, J. Zhang, P. Xiao, P.A. Webley, Int. J. Greenhouse Gas Control 1 (2007) 11–18.
[15] M. Tagliabue, D. Farrusseng, S. Valencia, S. Aguado, U. Ravon, C. Rizzo, A. Corma, C. Mirodatos, Chem. Eng. J. 155 (2009) 553–566.
[16] A. Saito, H.C. Foley, AIChE J. 37 (1991) 429–436.
[17] G. Horvath, K. Kawazoe, J. Chem. Eng. Jap. 16 (1983) 470–475.
[18] M.H. Kim, J.R. Ebner, R.M. Friedman, M.A. Vannice, J. Catal. 204 (2001) 348–357.
[19] M.H. Kim, J.R. Ebner, R.M. Friedman, M.A. Vannice, J. Catal. 208 (2002) 381–392.
[20] W.H. Yang, M.H. Kim, Korean J. Chem. Eng. 23 (2006) 908–918.
[21] J. McEwen, J.D. Hayman, A.O. Yazaydin, Chem. Phys. 412 (2013) 72–76.
[22] R.V. Siriwardane, M.S. Shen, E.P. Fisher, J.A. Poston, Energy Fuels 15 (2001) 279–284.
[23] J. Perez-Pellitero, H. Amrouche, F.R. Siperstein, G. Pirngruber, C. Nieto-Draghi, G. Chaplais, A. Simon-Masseron, D. Bazer-Bachi, D. Peralta, N. Bats, Chem. Eur. J. 16 (2010) 1560–1571.
[24] S. Sircar, Ind. Eng. Chem. Res. 45 (2006) 5435–5448.
[25] M. Radosz, X.D. Hu, K. Krutkramelis, Y.Q. Shen, Ind. Eng. Chem. Res. 47 (2008) 3783–3794.